PAGEOPH, Vol. 145, Nos. 3/4 (1995) 0033-4553/95/040647-30$1.50 + 0.20/0
© 1995 Birkhäuser Verlag, Basel

Interrelation between Fault Zone Structures and Earthquake Processes

KEIITI AKI[1]

Abstract—In order to develop capabilities for predicting earthquake processes on the basis of known fault zone structures and stress conditions, we need to find relations between seismogenic structures and processes. In the present paper we search for the scale dependence in various earthquake phenomena with the hope to find some structures in the earth that may control the earthquake processes. Among these phenomena, we shall focus on (1) geologic structures which play some role in nucleation and stopping of earthquake fault rupture, (2) depth ranges of the brittle seismogenic zone, (3) asperities and barriers distributed over a fault plane, (4) source-controlled f_{max} effect, (5) nonfractal behavior of creep events, and (6) temporal correlation between coda Q^{-1} and seismicity of earthquakes with magnitude characteristic to a given area. Our review of various scale-dependent phenomena leads us to propose a working hypothesis that the temporal change in coda Q^{-1} may reflect the activity of creep fractures near the brittle-ductile transition zone.

Key words: Seismogenic structure, coda Q^{-1}.

Introduction

Earthquakes are difficult subjects of scientific study, because they do not happen very often. Nevertheless, seismologists have accumulated knowledge about what happens during an earthquake and explained it quantitatively in terms of dynamic rupture of a geologic fault.

What we really want, however, is a predictive capability that will tell what will happen when a geologic fault with a known structure is subjected to a known stress condition. Unfortunately, the fault zone structure is very elusive. A cursory look at earthquake processes would lead you to conclude that earthquakes are chaotic, and self-similar, constrained primarily by its own size only.

In the present paper, we search for the scale-dependence in earthquake phenomena with the hope to find some structures in the earth that may control the earthquake processes. By the scale-dependence in earthquake phenomena, we mean

[1] Department of Earth Sciences, University of Southern California, Los Angeles, CA 90089-0740, U.S.A.

the existence of a unique length influencing earthquake phenomena in a given region. For example, the maximum earthquake in a region may be due to the repeated breaking of a fixed segment of a major fault in the region. In this case, the segment length uniquely determines the maximum earthquake of the region. Such an earthquake unique to a fault segement is called "characteristic earthquake" (SCHWARTZ and COPPERSMITH, 1984).

In this paper, we shall discuss a hierarchy of length scales relevant to earthquake phenomena ranging from the order of 100 km to that of 100 m. We shall start with the longest scale related to the irregularities of geometry of the plate boundary or major fault, which may control the nucleation and stopping points of an earthquake rupture. The width or depth of the brittle zone in the lithosphere may be another important length scale affecting the rupture propagation. We then discuss asperities and barriers that are responsible for strong ground motion generation. At the shortest scale, we shall address the issue of source-controlled f_{max}, the upper limit frequency generated by a given fault, in terms of the breakdown zone.

Finally, we present evidence for the existence of a unique structural unit in the brittle-ductile transition zone from the nonfractal distribution of creep events and the strong temporal correlation between the coda Q^{-1} and the relative frequency of earthquake with a certain magnitude specific to a given region. We consider the latter evidence most important because it is, perhaps, the only direct temporal correlation known between a structural parameter (Q^{-1}) and a seismicity parameter. We shall, therefore, review this evidence in a great detail.

Nucleation and Stopping of Fault Rupture

Let us start with a review of earthquakes for which the starting and stopping points of rupture propagation are known from seismological studies and maps of fault traces are available from geological studies. We found 24 such earthquakes as listed in Table 1.

A segment of the San Andreas fault for which the idea of characteristic earthquake may be supported from the evidence available from historic data (BAKUN and MCEVILLY, 1984) is the segment where the Parkfield earthquake of 1966 originated. It is widely accepted that the rupture for this characteristic earthquake nucleated near the Middle Mountain where the fault trace shows a slight bend of 3° to 5°. The bend is very subtle, and there is no step or branching associated with it.

The stopping point of the Parkfield earthquake of 1966 is believed by some (e.g., LINDH and BOORE, 1981) to be the right step in the Cholame Valley. We believe, however, that the rupture skipped the step in the manner similar to that found in the numerical simulation of DAS and AKI (1977) because there were aftershocks along the segment south of the step (EATON *et al.*, 1970) and the

Table 1

List of earthquakes

Name of earthquake	Data	Starting point type	Stopping point type	Reference
Fort Tejon	9 Jan. 1857	1	2	SIEH (1978,a,b)
San Francisco	18 Apr. 1906	2	1	BOLT (1968) BOORE (1977)
North Anatolia	26 Dec. 1939	1	2	DEWEY (1977)
Imperial	18 May 1940	1	2	RICHTER (1958)
North Anatolia	26 Nov. 1943	1	2	DEWEY (1976)
North Anatolia	1 Feb. 1944	1	2	DEWEY (1976)
Alaska	28 Mar. 1964	2	2	BURK (1965) KANAMORI (1970), KELLEHER and SAVINO (1975)
Parkfield	28 Jun. 1966	1	2	LINDH and BOORE (1981), AKI (1979)
Borrego Mountain	9 Apr. 1968	1	1	CLARK (1972), ALLEN and NORDQUIST (1972)
Guatemala	4 Feb. 1976	1	2	KANAMORI and STEWART (1978) PLAFKER, *et al.* (1976)
Gazli	8 Apr. 1976	1	2	HARTZELL (1980)
Gazli	17 May 1976	2	1	HARTZELL (1980)
Tangshan	27 Jul. 1976	1	2	BUTLER *et al.* (1979)
Izu-Oshima	14 Jan. 1978	1	2	SHIMAZAKI and SOMERVILLE (1979)
Coyote Lake	6 Aug. 1979	1	2	BOUCHON (1982), REASENBERG and ELLSWORTH (1982)
Imperial Valley	15 Oct. 1979	1	2	SHARP *et al.* (1982), ARCHULETA (1984)
Ghaenat	14 Nov. 1979	2	1	HAGHIPOUR and AMIDI (1980)
Ghaenat	27 Nov. 1979	2	1	HAGHIPOUR and AMIDI (1980)
El Asnam	10 Oct. 1980	1	2	DESCHAMPS *et al.* (1982) YIELDING *et al.* (1982)
Southern Italy	23 Nov. 1980	2	1	CROSSON *et al.* (1986), DESCHAMPS and KING (1983), DEL PEZZO *et al.* (1983)
Borah Peak	28 Oct. 1983	2	2	BRUHN *et al.* (1988)
Morgan Hill	24 April 1984	2	?	HARTZELL and HEATON (1986)
Superstition Hills	25 Nov. 1987	2	1	NICHOLSON (1988)
Landers	28 Jun. 1992	1	1	

displacement recorded at Station 2 of the Cholame strong motion seismograph array near the segment indicated strong evidence for the passage of a rupture front near the station (AKI, 1968, 1979; BOUCHON, 1979). The Cholame Valley step might have decelerated the rupture, but the final stopping of the rupture occurred at the branching point at which the San Juan fault (a Quaternary fault according to Jennings, 1975) meets the San Andreas fault. Recent analysis of geodetic data by SEGALL and DUS (1993) provides additional support to this interpretation. In either case, we identify the stopping point with a step or a branch point.

In order to make a systematic survey of geometric features of faults associated with the starting and stopping of rupture, we shall classify the geometry of a fault zone into the following two types guided by the prototype example of the Parkfield earthquake.

Type1: The fault trace is straight with or without a slight bend.

Type 2: The fault is significantly bent (10° or more), stepped, or branched.

Obviously, the starting point of the Parkfield earthquake belongs to type 1, and the stopping point to type 2.

For the other 23 earthquakes, we are able to classify the starting and stopping points into the above two types from the information available in the references listed in Table 1, except for the stopping point of the Morgan Hill earthquake.

The resultant statistics is as follows: a) in 15 cases out of 24 the starting point is associated with the type 1 feature; and b) in 15 cases out of 23 the stopping point is associated with the type 2 feature. In other words, we find a straight fault trace with or without a slight bend at about 63% of the starting points, and a significantly bent, stepped or branched fault trace at about 65% of the stopping points.

As mentioned earlier, the Parkfield earthquake is the prototype case in which the starting point is of type 1 and the stopping point is of type 2.

We found that 3 North Anatolian earthquakes, 2 Imperial Valley earthquakes, Fort Tejon, Guatemala, the first shock of Gazli, Tangshan, Izu-Oshima, Coyote Lake and El Asnam are of the same type. Including the Parkfield earthquake, this type occurs in 13 out of 24 cases.

The majority case noted above can be explained in terms of fracture mechanics. The fault trace of type 1 is simpler than that of type 2. The fracture energy required per unit area of the fault plane is expected to be less for the former than the latter. When a fault is under stress, the failure would initiate at the weakest part of the fault, namely, at a point of type 1. When the rupture encounters a point of type 2, which acts as a strong barrier, it will be stopped.

On the other hand, a significant bend, step or branch classified as type 2 can act as a stress concentrator. In this case, the rupture may nucleate at a point of type 2. The nucleation of rupture seems to have occurred in this manner for the 1906 San Francisco earthquake (near the branch point of the Palo Colorado San Gregorio fault), the 1964 Alaska earthquake (a corner of a plate boundary), Morgan Hill, Borah Peak, the second shock of Gazli, two Ghaenat earthquakes, Southern Italy

and the Superstition Hills. The latter five earthquakes are quite similar to each other in that the rupture nucleated near the crossing point of a conjugate fault.

The termination of rupture occurs at a point of type 1 for the 1906 San Francisco earthquake, Borrego Mountain, the second shock of Gazli, two Ghaenat earthquakes, Southern Italy, Superstition Hills and Landers earthquakes. In these cases, the rupture seems to stop because of running out of gas (driving stress).

Width of the Brittle Seismogenic Zone

SHIMAZAKI (1986) studied the relation between seismic moment and fault length for intraplate (mid-plate) earthquakes in Japan and recognized different relations for earthquakes with moments greater and smaller than about 7.5×10^{25} dyne cm. The moment is proportional to L^3 for the smaller ones and to L^2 for the larger ones. He explained the observed difference by the fault width constrained by the finite brittle zone for the larger ones, while the unconstrained self-similarity applies to the smaller ones.

Another interesting observation on the possible influence of the depth range of brittle zone derives from a rheological study of subduction zone earthquakes. SHIMAMOTO *et al.* (1993) subdivided a subducting plate boundary into three zones, namely (1) shallow aseismic zone where a massive solution-transfer takes place due to abundant H_2O, (2) brittle seismogenic zone, and (3) deeper ductile zone. Assuming that the boundary between (2) and (3) may be primarily determined by temperature, they estimated the width of the seismogenic zone at various subducting plate boundaries using the thermal structures, estimated by HONDA and UYEDA (1983). They found a good positive correlation between the estimated width of seismogenic zone and typical magnitude of thrust-type earthquakes in the subduction zone (KANAMORI, 1978; RUFF and KANAMORI, 1980). For example, the relative small size of thrust-type earthquakes in Mariana and New Hebrides is attributed to the narrow seismogenic zone with the width around 10 km, while great earthquakes in Chile are attributed to broad seismogenic zone with the width of a few hundred km.

Asperities and Barriers Distributed over a Fault Plane

The length scales discussed so far are related to the end points of earthquake rupture. We now discuss the length scales smaller than that of the entire fault, which are responsible for the irregularity of rupture propagation and the heterogeneity of slip distribution. The concepts of asperities and barriers have been introduced to describe such effects.

Recently AKI (1992) applied both asperity and barrier models to the observations on strong ground motions from major California earthquakes, and preferred the barrier model to the asperity model for the following three reasons. First, an

idealized asperity model cannot explain the observed sharp impulsive displacement perpendicular to the fault trace. Secondly, the observed complementary relation between fault slip and aftershocks supports the barrier model. Thirdly, evidence for the existence of barriers can be seen in the observations made by BAKUN *et al.* (1980) for the M5 characteristic earthquakes in the so-called creeping zone of the San Andreas fault.

Summarizing the results of applying the specific barrier model of PAPAGEORGIOU and AKI (1983) to major California earthquakes including the Loma Prieta earthquake studied by CHIN and AKI (1991), AKI (1992) found a systematic decrease in the barrier interval with decreasing magnitude. This is because of the peculiar scaling relation among major California earthquakes that the decrease in magnitude (or moment) is primarily due to the decreasing slip, and the relative constancy of local stress drop needed to explain observed strong motion demands smaller size subevent for smaller magnitude.

Interestingly, if we extrapolate the systematic relation between the barrier interval and magnitude to the creeping zone, we find that the subevent size for the characteristic earthquake ($M \simeq 5$) in the creeping zone is a few hundred meters, comparable to the size of breakdown zone inferred from the source-controlled f_{max} also extrapolated from major California earthquakes. Since the subevent size cannot be smaller than the breakdown zone size the creeping zone represents an end member of the family of major California earthquakes.

Source-Controlled f_{max}

PAPAGEORGIOU and AKI (1983) found that the shape of acceleration power spectra of observed strong motion for major California earthquakes departs from the flatness expected for the ω-squared model and starts decaying sharply beyond a cut-off frequency. This practical upper-limit frequency was called f_{max} by HANKS (1982), and was attributed to the effect of absorption by the near-surface earth. ANDERSON and HOUGH (1984) found that the effect can be explained by a layer of finite thickness with constant Q-type attenuation called the κ effect, and κ was in general greater for sediment sites than rock sites. The κ effect is clear at very high frequencies, but may not be significant (at least for weak motion) in the frequency range below 12 Hz, because SU *et al.* (1992) found higher site amplification for sediment sites than for rock sites in this frequency range. Whether the f_{max} is due to source or site effects has been difficult to resolve.

Originally, PAPAGEORGIOU and AKI (1993) attributed f_{max} to the source effect, without considering the site effect. Later, PAPAGEORGIOU (1988) showed that f_{max} was not significantly different between a soil site and a rock site in the case of the San Fernando earthquake. Nevertheless, AKI and PAPAGEORGIOU (1989) applied the site effect correction based on the results of PHILLIPS and AKI (1986), and still

found the source-controlled f_{max} effect although revised to be increased by a factor of 2 than the original estimate.

Recently, CHIN and AKI (1991) considered simultaneously the source, path and site effects on the acceleration power spectra of the strong motion during the Loma Prieta earthquake of 1989, and obtained f_{max} after eliminating the site and propagation path effects. The value of f_{max} obtained for the Loma Prieta earthquake was consistent with the f_{max}-magnitude relation obtained earlier for other major California earthquakes. f_{max} shows a slight decrease with magnitude; about 10 Hz for $M6$ to 5 Hz for $M7.5$.

A similar decrease in f_{max} with magnitude was observed by IRIKURA and YOKOI (1984) for earthquakes in Japan, and by ROCA (1990) for earthquakes in Taiwan.

GUSEV (1992) calculated Fourier spectra of strong motion from the East Kamchatka earthquake of December 15, 1971 ($M = 7.8$) recorded at station Krutoberegovo, which showed a clear f_{max} at 2 to 3 Hz, which cannot be attributed to a local site effect.

Most convincing evidence for the source-controlled f_{max} effect comes from a recent work by KINOSHITA (1992) who found that acceleration Fourier spectra obtained by seismographs placed in the basement rock at about 3 km depth show distinctly different f_{max} (below 10 Hz to more than 30 Hz) depending on the hypocenter location. The lowest f_{max} was found for earthquakes occurring in the region where the Pacific Plate and the Philippine Sea Plate are in contact. It is also low for shallow earthquakes in the volcanic region.

If f_{max} is due to the source effect, it must represent some kind of smoothing the seismic radiation. The time constant of smoothing, namely $1/f_{max}$, may correspond to the spatial smoothing constant d of v/f_{max}, where v is the rupture velocity. For $v = 3$ km/s the range of f_{max} from 3 Hz to 10 Hz, corresponds to the range of d from 1 km to 300 m. PAPAGEORGIOU and AKI (1993) related d to the size of cohesive zone, or breakdown zone. The above-mentioned magnitude dependence of f_{max} implies the larger breakdown zone for the greater earthquake.

The above cohesive zone, or breakdown zone may be related to the low-velocity low-Q zone discovered by recent observations on seismic guided waves trapped in the fault zone of the Oroville earthquake of 1975, the San Andreas fault near Parkfield and the Landers earthquake of 1992 (LEARY *et al.*, 1987; LI and LEARY, 1990; LI *et al.*, 1990, 1994a,b).

For example, the width of the low velocity (with shear wave velocity 2.0–2.2 km/s in contrast to the surrounding medium with 3.0 km/s) and low Q (about 50) zone of the Landers, California, earthquake fault was estimated to be about 180 m, comparable to the width of breakdown zone estimated from f_{max}.

Nonfractal Behavior of Creep Events

Evidence for aseismic creep on the San Andreas fault was discovered in 1956 during an investigation of damage at Cienega Winery (STEINBRUGGE *et al.*, 1960).

Efforts to obtain continuous creep records there were begun in 1958 (TOCHER, 1960), and extended to many sites along the San Andreas fault in central California, as reviewed by BURFORD (1988).

A typical creep record consists of a sequence of quasi-periodic creep events, each of which appears to show a step-like slip with amplitude on the order of 1 mm, although occasional events with amplitude exceeding 10 mm also occur. We measured the amplitude of step-like change in a creep event for three sites (CWC3, CWN1, and XMR1) selected from BURFORD (1988). The distribution of the amplitude followed the normal distribution very well, and clearly deviated from the power-law distribution. The clear failure of power law supports the nonfractal nature of creep events. The very good fit of the normal distribution strongly suggests the existence of a mean characateristic slip associated with them. This characteristic slip may correspond to the size of breakdown zone and that of subevents in the creeping zone as discussed in the preceding two sections.

Seismic Coda Waves

As mentioned in the introduction, we shall describe the relation between coda Q^{-1} and seismicity in a great detail, because it represents, perhaps, the only direct temporal correlation known between a structural parameter and a seismicity parameter. Let us start with introducing seismic coda waves, because they are not explained in any existing seismology text book.

When an earthquake occurs in the earth, seismic waves are propagated away from the source. After P waves, S waves and various surface waves are gone, the area around the seismic source is still vibrating. The amplitude of vibration is uniform in space, except for the local sites effect, which tends to amplify the motion at soft soil sites as compared to hard rock sites. This residual vibration is called seismic coda waves, and decays very slowly with time. The rate of decay is the same independent of the locations of seismic source and recording station, as long as they are located in a given region. An example of coda waves is shown in Figure 1. They are seismograms of a local earthquake near a seismic array in Norway constructed for monitoring the underground nuclear testing in USSR in early 1970s. The array aperture is about 100 km, and the epicentral distance is a few kilometers to the closest station, and more than 100 km to the farthest. In spite of the great difference in distance, which is of course reflected in arrival times and amplitudes of primary waves, the coda waves show a very similar amplitude and rate of decay among all stations. The signal is band-pass filtered around 4 Hz, and the coda last more than 200 seconds in this old stable part of the continent.

The closest phenomena to this coda wave is the residual sound in a room, first studied by SABINE (1922). If you shoot a gun in a room, the sound energy remains for a long time due to incoherent mutliple reflections. This residual sound has a very stable, robust nature similar to seismic coda waves, independent of the

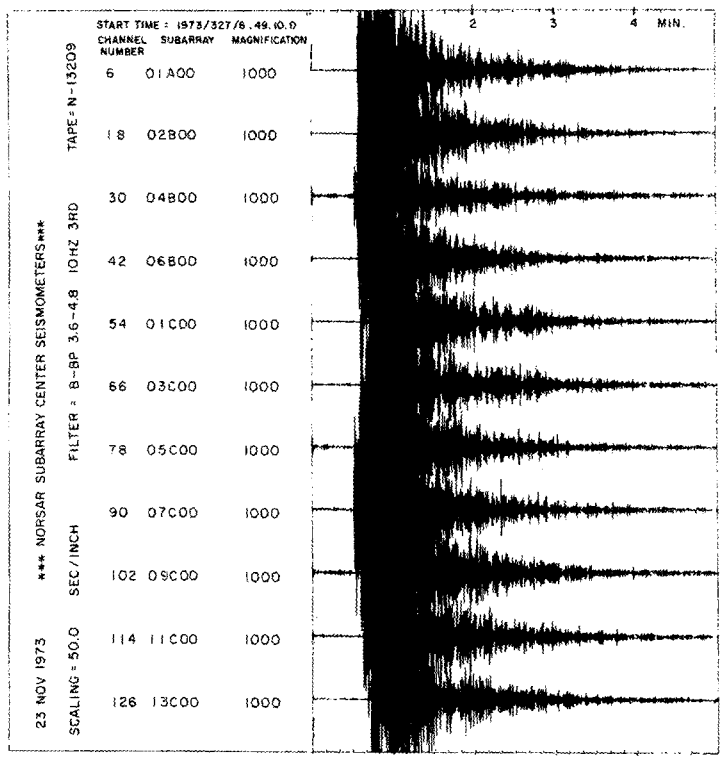

Figure 1
Short-period (band pass between 3.6 and 4.8 Hz) records of a local earthquake at Norsar near subarray 7C. The epicentral distance is a few kilometers to the closest station and more than 100 km to the farthest. The general level and decay rate of coda energy show no dependence on the epicentral distance.

locations where you shoot the gun or where you record the sound in the room. The residual sound remains in the room because of multiple reflections at rigid wall, ceiling and floor of the room. Since we cannot hypothesize any room-like structure in the earth, we attribute seismic coda waves to backscattering from numerous heterogeneities in the earth. We may consider seismic coda as waves trapped in a random medium.

The seismic coda waves from a local earthquake can be best described by the time-dependent power spectrum $P(\omega \mid t)$, where ω is the angular frequency and t is the time measured from the origin time of the earthquake. $P(\omega \mid t)$ can be measured from the squared output of a band-pass filter centered at a frequency ω, or from the squared Fourier amplitude obtained from a time window centered at t. The most extraordinary property of $P(\omega \mid t)$ is the simple separability of the effects of seismic source, propagation path and recording site response, expressed by the following equation. The coda power spectrum $P_{ij}(\omega \mid t)$ observed at the ith station due to the

jth earthquake can be written as

$$P_{ij}(\omega \mid t) = S_j(\omega)R_i(\omega)C(\omega \mid t) \tag{1}$$

for t greater than about twice the travel time of S waves from the jth earthquake to the ith station. Equation (1) means that $P_{ij}(\omega \mid t)$ can be written as a product of a term $S_j(\omega)$ which depends only on the earthquake source, a term $R_i(\omega)$ which depends only on the recording site and a term $C(\omega \mid t)$ common to all earthquakes and recording sites in a given region.

The above property of coda waves expressed by equation (1) was first recognized by AKI (1969) for aftershocks of the Parkfield, California earthquake of 1966. The condition that equation (1) holds for t greater than about twice the travel time of S waves was found by the extensive study of coda waves in central Asia by RAUTIAN and KHALTURIN (1978). Numerous investigators demonstrated the validity of equation (1) for earthquakes around the world, as summarized in a review article by HERRAIZ and ESPINOSA (1987). In general, equation (1) holds more accurately for a greater lapse time t and for higher frequencies (e.g., SU *et al.*, 1991). Coda waves are a powerful tool for seismologists because equation (1) offers a simple means to separate the effects of source, path and recording site. The equation has been used for a variety of practical applications, including the mapping of frequency-dependent site amplification factor (e.g., SU *et al.*, 1992), discrimination of quarry blasts from earthquakes (SU *et al.*, 1991), single station method for determining frequency-dependent attenuation coefficients (AKI, 1980), and normalizing the regional seismic network data to a common source and recording site condition (MAYEDA *et al.*, 1992).

In the following, we shall focus on the common decay founction $C(\omega \mid t)$ on the right-hand side of equation (1). We shall first introduce coda Q to characterize $C(\omega \mid t)$ in the framework of single-scattering theory, and then summarize the current results on what the coda Q is in terms of scattering attenuation and intrinsic absorption. Then, we shall survey the spatial and temporal variation in coda Q^{-1} and describe how they are related to earthquake processes in the lithosphere.

Introducing Coda Q (or Coda Q^{-1})

The first attempt to predict the explicit form of $P(\omega \mid t)$ for a mathematical model of earthquake source and earth medium was made by AKI and CHOUET (1975). Their models were based on the following assumptions.

(1) Both primary and scattered waves are S waves.
(2) Multiple scatterings are neglected.
(3) Scatterers are distributed randomly with a uniform density.
(4) Background elastic medium is uniform and unbounded.

The assumption (1) has been supported by various observations, such as the common site amplification (TSUJIURA, 1978) and the common attenuation (AKI,

1980) between S waves and coda waves. It is also supported theoretically because the S to P conversion scattering due to a localized heterogeneity is an order of magnitude smaller than the P to S scattering as shown by AKI (1992) using the reciprocal theorem. ZENG (1993) has shown that the above difference in conversion scattering between P to S and S to P leads to the dominance of S waves in the coda.

Since the observed $P(\omega \mid t)$ is independent of the distance between the source and receiver, we can simplify the problem further by co-locating the source and receiver. Then, we find (AKI and CHOUET, 1975, see also AKI, 1981 for more detailed derivation) that

$$P(\omega \mid t) = \beta/2g(\pi) \mid \phi_0(\omega \mid \beta t/2)^2 \tag{2}$$

where β is the shear wave velocity, $g(\theta)$ is the directional scattering coefficient, and $\phi_0(\omega \mid r)$ is the Fourier transform of the primary waves at a distance r from the source. $g(\theta)$ is defined as 4π times the fractional loss of energy by scattering per unit travel distance of primary waves and per unit solid angle at the radiation direction θ measured from the direction of primary wave propagation.

AKI and CHOUET (1975) adopted the following form for $|\phi_0(\omega \mid r)|$.

$$|\phi_0(\omega \mid r)| = |S(\omega)| r^{-1} \exp\left(-\frac{\omega t}{4Q_c}\right), \tag{3}$$

where $|S(\omega)|$ is the source spectrum, r^{-1} represents the geometrical spreading, and Q_c is introduced to express the attenuation.

Combining (2) and (3), and including the attenuation of scattered waves, we have

$$P(\omega \mid t) = \frac{2g(\pi)|S(\omega)|^2}{\beta t^2} \exp(-\omega t/Q_c). \tag{4}$$

Q_c is called "coda Q," and Q_c^{-1} is called "coda Q^{-1}."

The measurement of coda Q according to equation (4) is very simple. Coda Q^{-1} is the slope of straight line fitting the measured $\ln(t^2 P(\omega \mid t))$ vs. ωt. Since there is a weak but sometimes significant dependence of the slope on the time window for which the fit is made, it has become a necessary routine to specify the time window for each measured coda Q^{-1}.

Because of the simplicity of measurement of coda Q^{-1}, its geographical variation over a large area as well as its temporal variation over a long time can be studied relatively easily. Before presenting those results, however, we need to clarify what is the physical meaning of coda Q^{-1}.

Physical Meaning of Coda Q^{-1}

The physical meaning of Coda Q^{-1} has been debated for almost twenty years. Within the context of the single scattering theory, coda Q^{-1} appears to represent an effective attenuation including both absorption and scattering loss. This idea

prevailed for some time after AKI (1980) found a close agreement between coda Q^{-1} and Q^{-1} of S waves measured in the Kanto region, Japan. On the other hand, numerical experiments by FRANKEL and CLAYTON (1986), laboratory experiments by MATSUNAMI (1991), and theoretical studies including multiple scattering effects (e.g., SHANG and GAO, 1988) concluded that the coda Q^{-1} measured from the time window later than the mean free time (mean free path divided by wave velocity) should correspond only to the intrinsic absorption, and should not include the effect of scattering loss. The debates concerning this issue were summarized by AKI (1991).

In order to resolve the above issue, attempts have been made to separately determine the scattering loss and the intrinsic loss in regions where coda Q^{-1} has been measured. For this purpose, it is necessary to include multiple scattering in the theoretical model, either by the radiative energy transfer approach (WU, 1985) or by the inclusion of several multiple-path contributions to the single-scattering model (GAO *et al.*, 1983). Recently, ZENG *et al.* (1991) demonstrated that all these approaches can be derived as approximate solutions of the following integral equation for the seismic energy density $E(x, t)$ per unit volume at a location x and at time t due to an impulsive point source applied at x_0 at $t = 0$.

$$E(x, t) = E_0\left(t - \frac{|x - x_0|}{\beta}\right)\frac{e^{-\eta|x - x_0|}}{4\pi|x - x_0|^2} + \int_V \eta_s E\left(\xi, t - \frac{|\xi - x|}{\beta}\right)\frac{e^{-\eta|\xi - x|}}{4\pi|\xi - x|^2}\, dV(\xi) \tag{5}$$

where symbols are defined as follows:

$E(x, t)$: seismic energy per unit volume at x and t

η: total attenuation coefficient: $\eta = \eta_s + \eta_i$ (energy decays with distance $|x|$ as $\exp[-\eta|x|]$)

η_i: intrinsic absorption coefficient

η_s: scattering attenuation coefficient

$Q_s^{-1} = \dfrac{\eta_s \beta}{\omega}$: scattering Q^{-1}

$Q_i^{-1} = \dfrac{\eta_i \beta}{\omega}$: absorption Q^{-1}

$B = \dfrac{\eta_s}{\eta}$: albedo

$L_e = \dfrac{1}{\eta}$: extinction distance

$L = \dfrac{1}{\eta_s}$: mean free path

$\beta E_0(t)$: rate of energy radiated from a point source at x_0 at t.

The assumptions underlying equation (5) are less restrictive and more explicit than the assumptions used in deriving equations (2) and (4). The background medium is still uniform and unbounded, but scattering coefficients and absorption coefficients are explicitly specified, and all multiple scatterings are included, although scattering is assumed to be isotropic. Equation (5) gives the seismic energy density as a function of distance and time in contrast to equations (2) and (4) which depend on time only. By comparing the predicted energy density in space and time with the observed, we can uniquely determine the scattering loss and the intrinsic absorption, separately.

An effective method using the Monte-Carlo solution of equation (5) was developed by HOSHIBA *et al.* (1991) who calculated seismic energy integrated over three consecutive time-windows (e.g., 0 to 15, 15 to 30, 30 to 45 sec. from the S arrival time) and plotted them against distance from the source. The method has been applied to the various parts of Japan (HOSHIBA, 1993), Hawaii, Long Valley, California, central California (MAYEDA *et al.*, 1992), and southern California (JIN *et al.*, 1994).

Figure 2 shows typical examples of comparison between the predicted energy density and the observed. The observed energy density data come from many small earthquakes recorded at a single station, and are normalized to a common source by the coda normalization method of AKI (1980). In spite of the simplified assumptions made in the prediction, the comparison with the observations is quite good, giving us some confidence in the estimated scattering and absorption coefficients.

Figure 3 (JIN *et al.*, 1994) compares seismic albedo B_0, total attenuation coefficient η $(=1/Le)$ in km^{-1}, scattering coefficient η_s and intrinsic absorption η_i among Long Valley, central California, southern California, Hawaii, and Japan. Except for outlayers for Hawaii (at 1.5 and 3 Hz), which are probably due to inadequacy of model, the scattering and attenuation of seismic waves in the frequency range from 1 to 25 Hz are remarkably consistent in all these regions.

First, η_s tends to decrease with increasing frequency. This corresponds to the decrease of Q_s^{-1} faster than f^{-1} with increasing frequency f. In terms of the random medium model, this implies that the autocorrelation function may be more like Gaussian rather than exponential (SATO, 1982a,b; WU, 1982; FRANKEL and CLAYTON, 1986). The Gaussian type medium shows much smoother variation than the exponential type below the correlation distance. There appears to be no difference between geothermal areas such as Hawaii and Long Valley and primarily nongeothermal active areas such as central and southern California.

Figure 3 also exhibits that the intrinsic absorption η_i shows a slight increase with increasing frequency. Because of the opposite frequency dependence of η_s and η_i, the intrinsic absorption dominates the scattering at higher frequencies. Thus, the seismic albedo B_0 shown in Figure 3 is less than 0.5 for all areas at frequencies higher than 5 Hz. At lower frequencies, we found large regional variation in B_0.

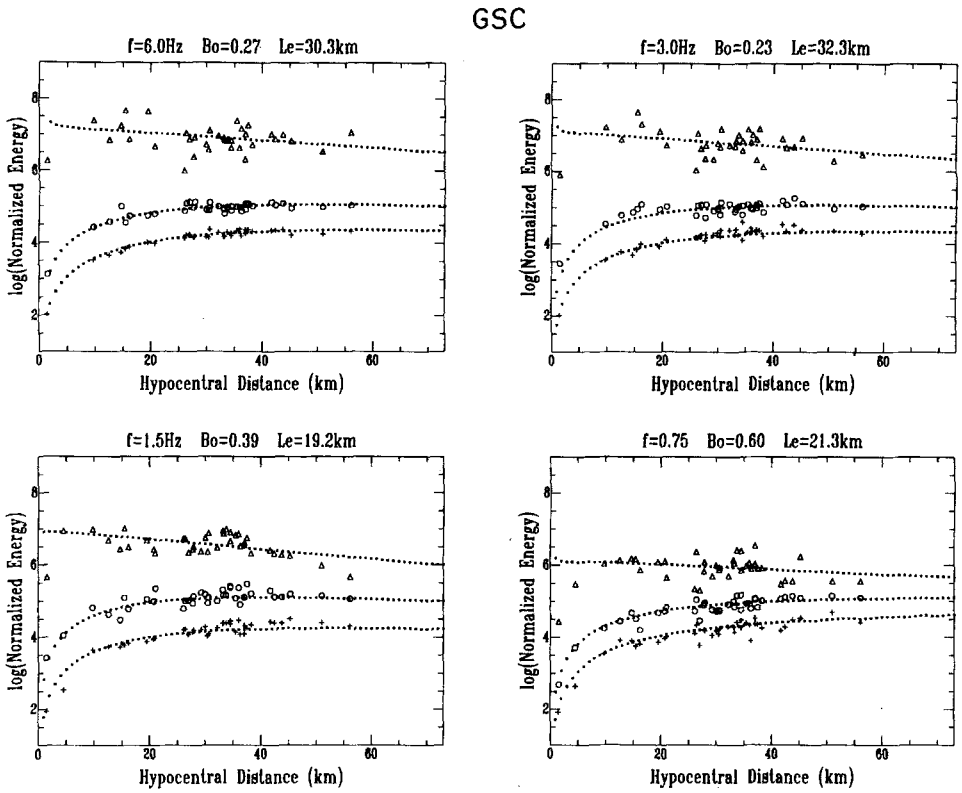

Figure 2
Observed coda energy in 4 frequency bands in three consecutive lapse time windows (triangle: 15 sec. from S arrival, circle: 15 to 30 sec., and cross: 30 to 45 sec.) at station *GSC* in southern California normalized by the coda method. The dotted curves represent the prediction for best-fitting parameters. The center frequency f of the band, albedo B_0, and extinction distance Le are shown above each figure.

Now that we have several regions where intrinsic Q and absorption Q have been determined, we can compare the coda Q with them. Figure 4 shows Q_i^{-1}, Q_s^{-1} and Q_t^{-1} $(=Q_i^{-1}+Q_s^{-1})$ as a function of coda Q^{-1} separately for Hawaii, southern California, central California, Long Valley and Japan. The coda Q^{-1} is determined for the lapse time interval 20 to 45 s for southern California, 30 to 60 s for Long Valley, Hawaii and central California, and 20 to 60 s for Japan. In general, coda Q^{-1} lies between Q_i^{-1} and Q_t^{-1}. It is closer to Q_i^{-1} for Japan, and closer to Q_t^{-1} for all other regions. According to GAO and AKI (1994), who made a numerical study of the departure of coda Q^{-1} and Q_i^{-1} for models of a scattering layer with a finite thickness, the above results may indicate that the thickness of scattering layer is greater than the mean free path under Japan, but comparable or smaller than the mean free path for the other regions.

Although, for a more complete understanding of coda Q, we need models with nonuniform scattering and absorption coefficients. Figure 4 assures us empirically

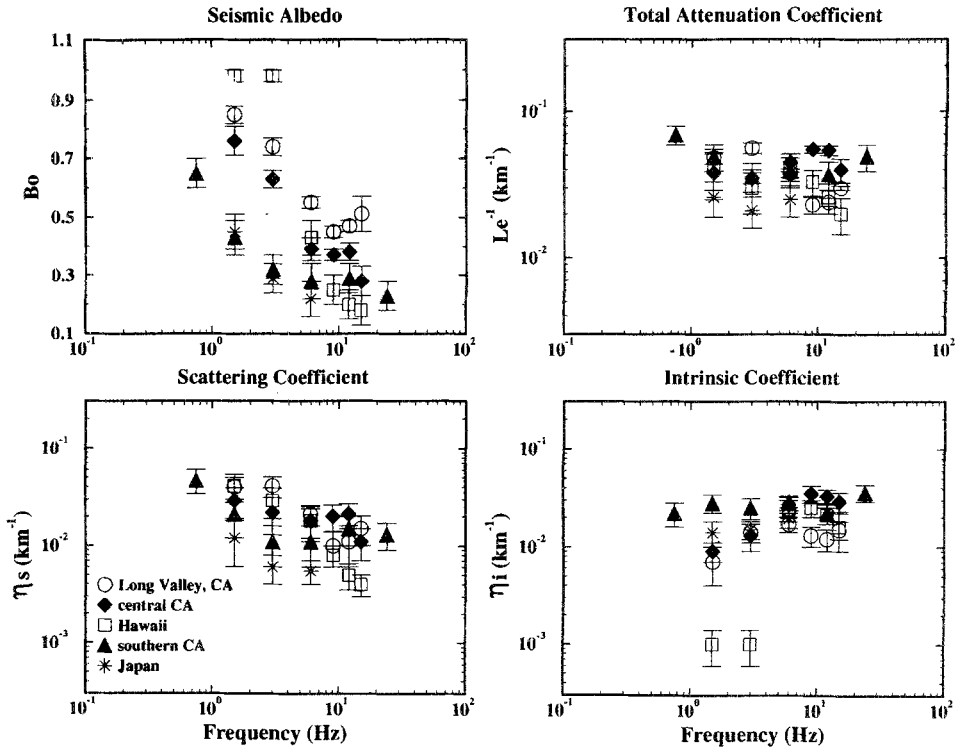

Figure 3
Albedo B_0, total attenuation coefficient $\eta(-1/Le)$, scattering coefficient η_s and intrinsic absorption η_i as a function of frequency for various regions.

that coda Q^{-1} are bounded rather narrowly between intrinsic and total Q^{-1}. With this understanding of coda Q^{-1}, we shall now proceed to the spectacular spatial and temporal correlation observed between coda Q^{-1} and seismicity.

Geographic Variation in Coda Q

The decay rate of coda waves shows a strong geographic variation. The example from Norway, an old stable region, given in Figure 1 clearly shows a very high Q because the duration of 200 seconds for 4 Hz means 800 cycles of vibration. On the other hand, the coda decay considerably more quickly in young active regions, such as Japan and California. For example, SINGH and HERRMANN (1983) found a systematic variation of coda Q at 1 Hz in the conterminous U.S.: more than 1000 in the central part decaying gradually to 200 in the western U.S.

The spatial resolution of the map of coda Q obtained by SINGH and HERRMANN (1983) was rather poor, because they had to use distant earthquakes to

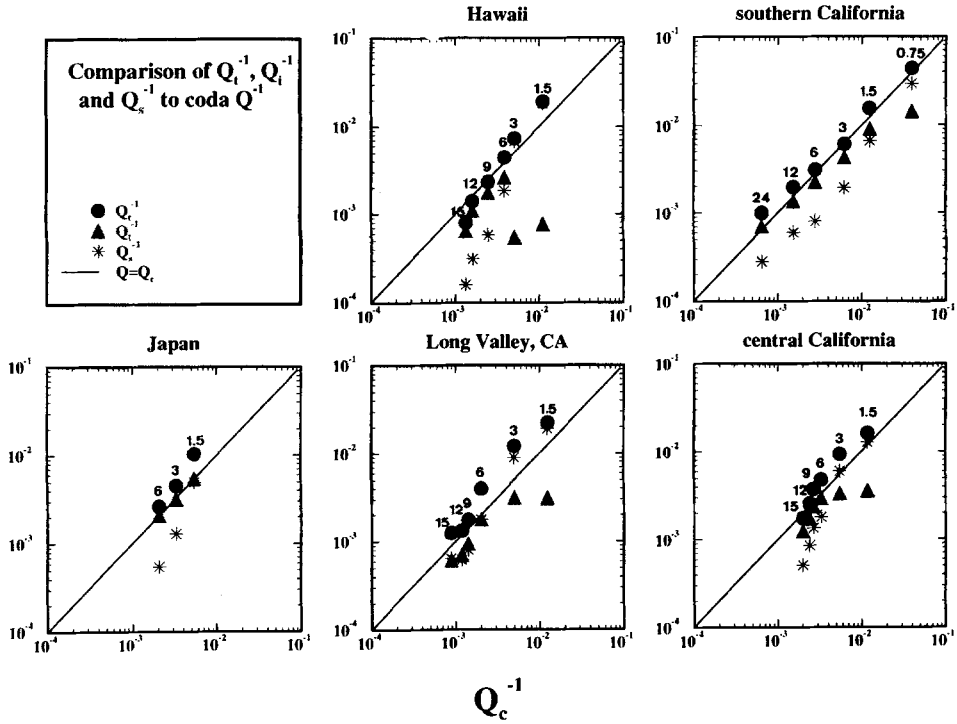

Figure 4
Comparison of coda Q^{-1} (Q_c^{-1}) with scattering Q^{-1} (Q_s^{-1}), intrinsic Q^{-1} (Q_c^{-1}) and total Q^{-1} (Q_t^{-1}) at various frequencies for five regions.

cover regions of low seismicity. As mentioned earlier, equation (1) holds for the lapse time to greater than about twice the travel time for S waves. For a more distant earthquake, the coda part governed by equation (1) starts later, making the region traveled by waves composing the coda greater and consequently losing the spatial resolution.

PENG (1989) made a systematic study of the spatial resolution of coda Q mapping as a function of the lapse time window selected for measuring coda Q. He used the digital data from the Southern California Seismic Network operated by Caltech and USGS, and calculated spatial autocorrelation function of coda Q^{-1} by the following procedure. Southern California is divided into meshes of size 0.2° (longitude) by 0.2° (latitude), and the average of coda Q^{-1} is calculated for each mesh using seismograms which have the mid-point of epicenter and station in the mesh. The average value for the ith mesh is designated as χ_i. Then two circles of radius r and $r + 20$ km are drawn with the center at the ith mesh, and the mean of coda Q^{-1} at mid-points located in the ring between the two circles is calculated and designated as $y_i(r)$. The autocorrelation coefficient $\rho(r)$ is computed by the

following formula,

$$\rho(r) = \frac{\sum_{i=1}^{M} (x_i - \bar{x})(y_i(r) - \bar{y}(r))}{\sqrt{\sum_{i=1}^{M} (x_i - \bar{x})^2} \sqrt{\sum_{i=1}^{M} (y_i(r) - \bar{y}(r))^2}}$$

where, M is the total number of meshes, $\bar{x}$ is the mean of x_i, and $\bar{y}(r)$ is the mean of $y_i(r)$. $\rho(r)$ is calculated for coda Q^{-1} at four different frequencies (1.5, 3, 6 and 12 Hz) and three different lapse time windows, namely, 15 to 30 sec., 20 to 45 sec. and 30 to 60 sec. measured from the origin time. As shown in Figures 5 through 7, the autocorrelation functions are similar among different frequencies, but depend clearly on the selected time window. The longer and later time window gives the slower decay in the autocorrelation with the distance separation. If we define the distance at which the correlation first comes close to zero as the "coherence distance," the average coherence distance is about 135 km for time window 30–60 sec., 90 km for the window 20–45 sec., and 45 km for the window 15–30 sec.

The above observation offers a strong support to the assumption that coda waves are composed of S to S backscattering waves, because the distance traveled by S waves with a typical crustal S wave velocity of 3.5 km/s in half the lapse time 60, 45 and 30 sec. are, respectively, 105, 79 and 53 km, which are close to the corresponding coherence distance, namely, 135, 90 and 45 km. In other words, the coda Q^{-1} measured from a time window represents the seismic attenuation

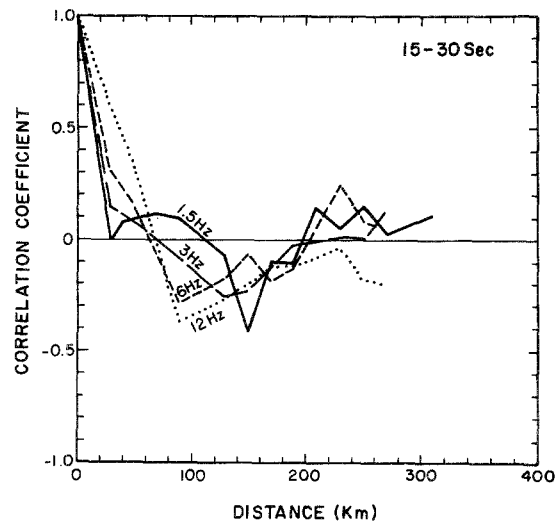

Figure 5
Spatial autocorrelation function of coda Q^{-1} at various frequencies measured from the time window 15–30 sec. in southern California obtained by PENG (1989).

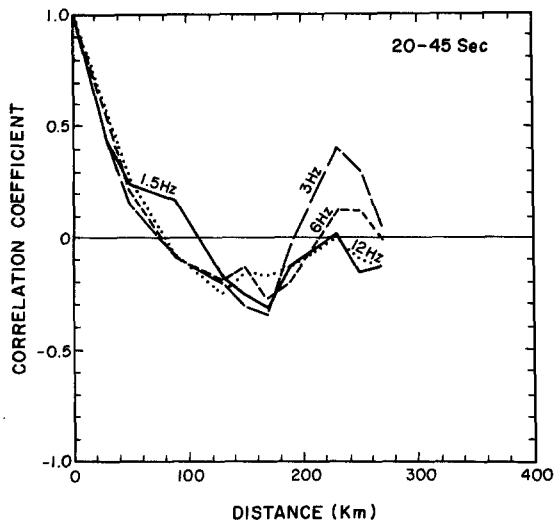

Figure 6
Spatial autocorrelation function of coda Q^{-1} at various frequencies measured from the time window 20–45 sec. in southern California obtained by PENG (1989).

property of the earth's crust averaged over the volume traversed by the singly backscattering S waves.

JIN and AKI (1988) were able to construct a map of coda Q at 1 Hz for the mainland China with a high spatial resolution using earthquakes at short distances from each station as shown in Figure 8. The coda Q at individual stations estimated

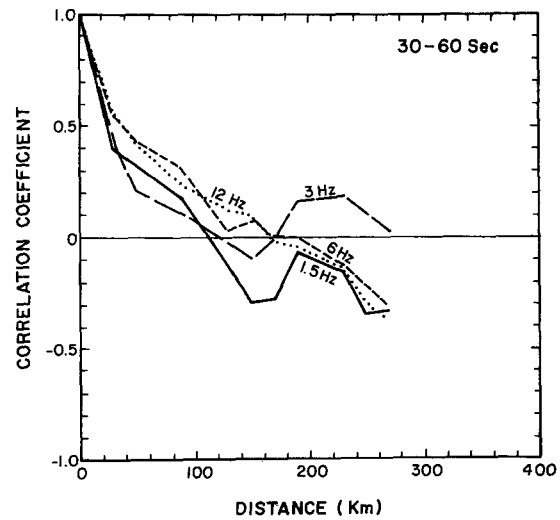

Figure 7
Spatial autocorrelation function of coda Q^{-1} at various frequencies measured from the time window 30–60 sec. in southern California obtained by PENG (1989).

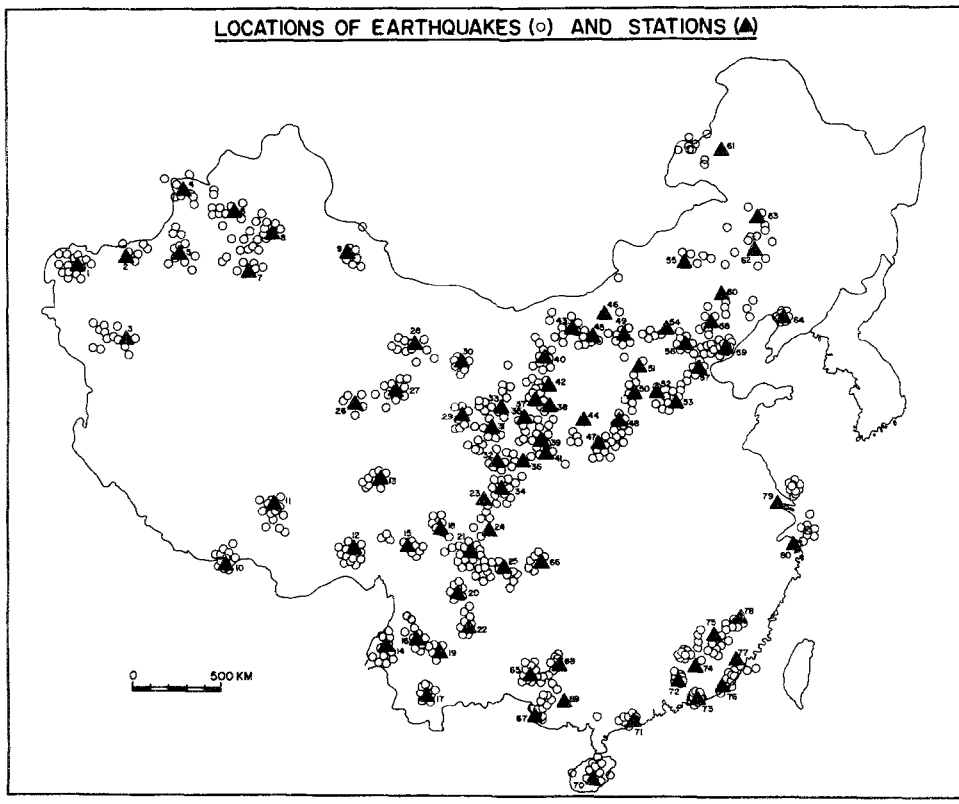

Figure 8
Location of earthquakes (circles) and stations (cross) used by JIN and AKI (1988).

from these earthquakes for the time window from $2t_s$ to 100 sec., shown in Figure 9, where the variation is smooth enough to draw contours of equal coda Q. The contour map of coda Q is compared with epicenters of major earthquakes with $M \geqq 7$ in Figure 10. A strong correlation was found between coda Q and seismicity. Seismically active regions, such as Tibet, western Yunnan and North China, correspond to low coda Q region, and stable regions such as Ordos plateau, middle-eastern China, and the desert in southern Xinjiang have very high coda Q. The difference between the highest coda Q value and the lowest amounts to more than a factor of 20. Thus, mapping coda Q can be useful for the assessment of long-term seismic hazard.

Two different symbols are used to distinguish earthquakes that occurred before 1700 from those that occurred after 1700. As well known among Chinese seismologists, there has been a migration of epicenters from west to east during the past 300 years in North China. It is interesting to note that the coda Q values for the region active before 1700 is about twice as high as those for the region currently active. JIN and AKI (1988) suggests that the low coda Q region might also have migrated

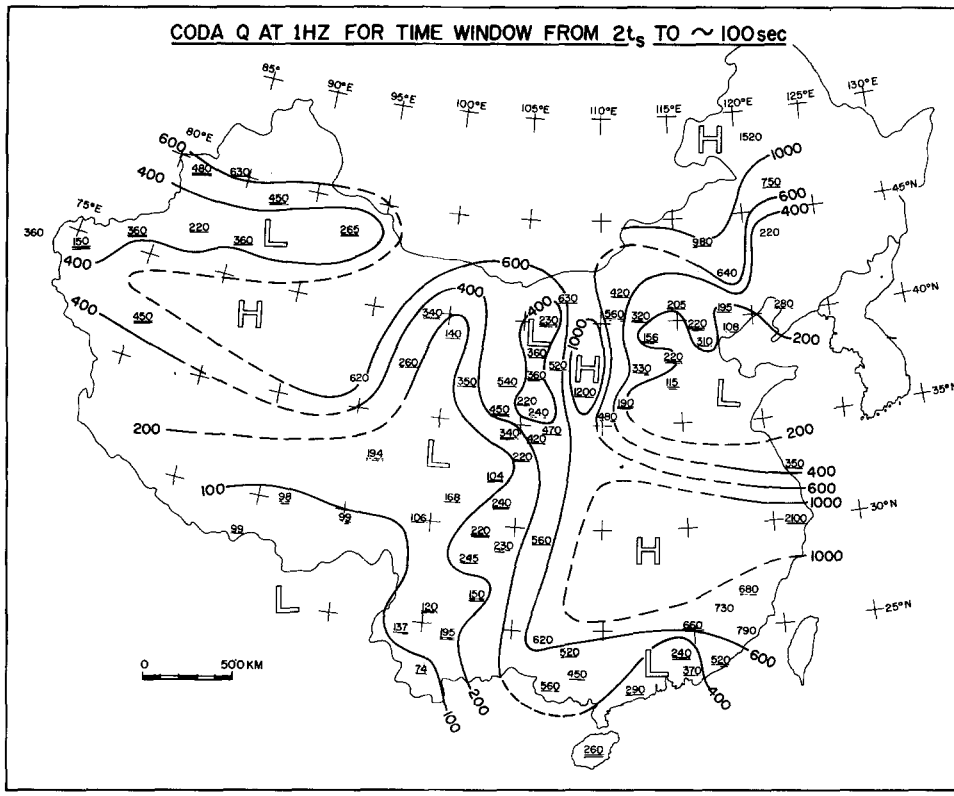

Figure 9
Measured coda Q values at 1 Hz with time window from $2t_s$ (S-wave travel time) to 100 sec. and the iso-Q lines, adapted from JIN and AKI (1988).

together with the high seismicity, referring to the Q values estimated by CHEN and NUTTLI (1984a,b) from intensity maps for past major earthquakes in the region. This leads us to the most intriguing observation on coda Q, namely, its temporal change.

Temporal Change in Coda Q

CHOUET (1979) was the first to observe a significant temporal change in coda Q at Stone Canyon, California, which could not be attributed to changes in instrument response, or in the epicenter locations, focal depths, or magnitudes of earthquakes used for the measurement. The change was associated with neither the rainfall in the area nor with the occurrence of any particular earthquake, but showed a weak negative correlation with the temporal change in a seismicity parameter called "b-value" (AKI, 1985). The b-value is defined in the Gutenberg-

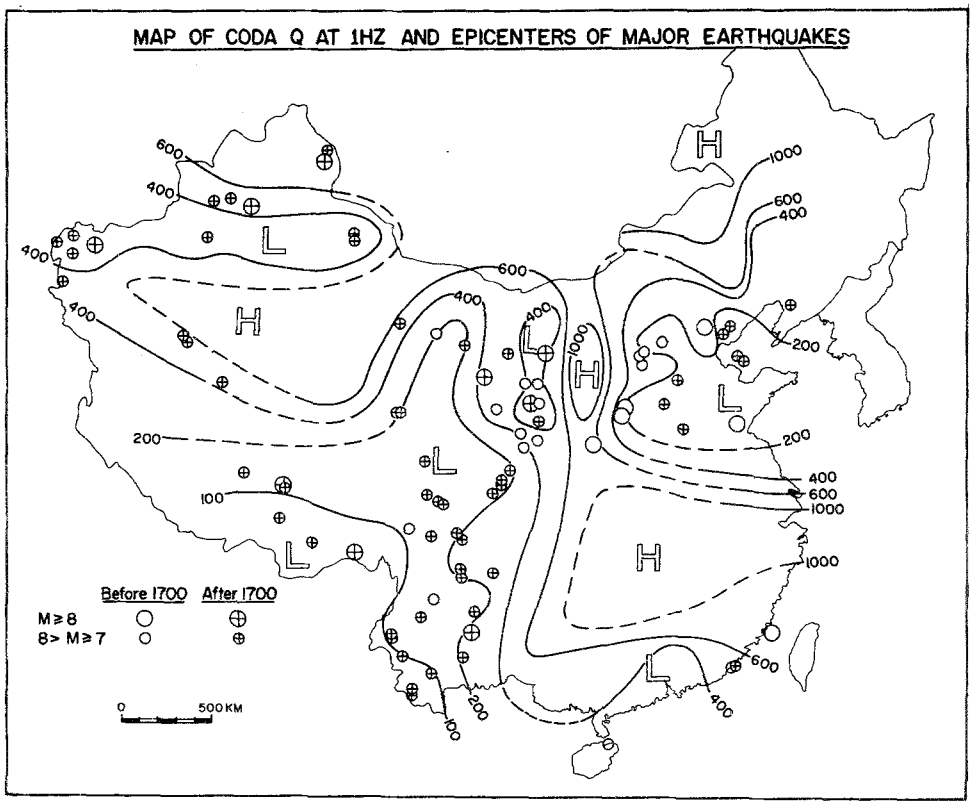

Figure 10
Map of coda Q at 1 Hz and epicenters of major earthquakes with $M \geq 7$. Different symbols are used for $M \geq 8$ and $M < 8$, and before and after 1700, adapted from JIN and AKI (1988). The high Q regions are devoid of earthquakes, and the low Q regions are full of them.

Richter formula $\log N = a - bM$, where N is the frequency of earthquakes with magnitude greater than M.

Numerous studies made since (see SATO, 1988 for a critical review of early works) revealed that the temporal correlation between coda Q^{-1} and seismicity is not as simple as the spatial correlation described in the preceding section.

In a number of cases (GUSEV and LEMZIKOW, 1984; NOVELO-CASANOVA *et al.*, 1985; JIN and AKI, 1986; SATO, 1986; FAULKNER, 1988; SU and AKI, 1990), coda Q^{-1} shows a peak during a period of 1–3 years before the occurrence of a major earthquake. A similar precursory pattern showed up also before the 1989 Loma Prieta earthquake in central California, and the Landers earthquake in southern California (JIN and AKI, 1993). From the study of coda Q^{-1} over the period more than 50 years for both central and southern California, as shown in Figure 11 where $\beta_0 = \pi f Q_c^{-1}$ is plotted as a function of time, JIN and AKI (1993) had to conclude that the coda Q^{-1} precursor is not reliable, because a similar pattern,

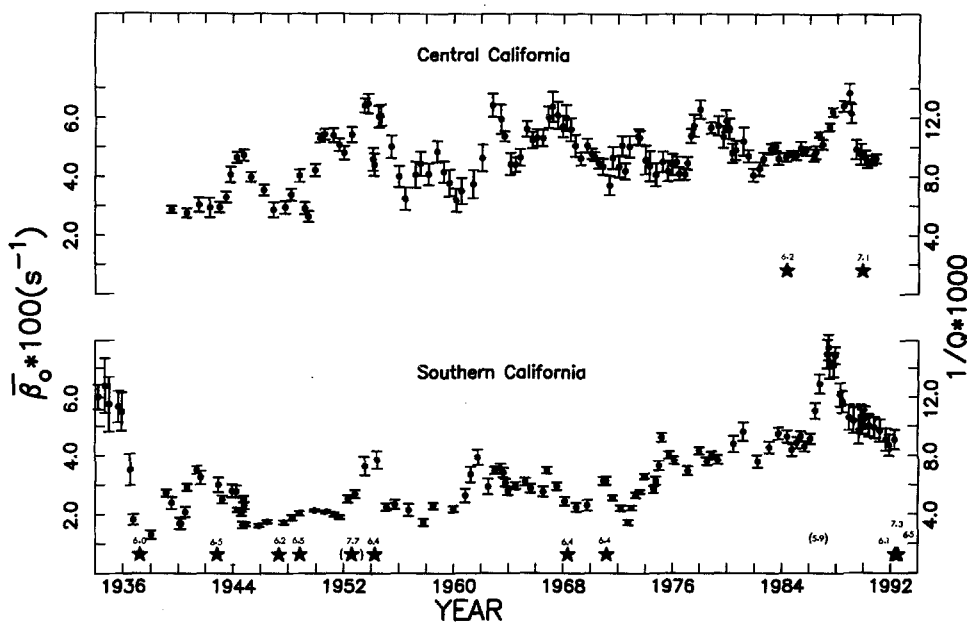

Figure 11
Mean values of $\beta_0 = \pi f Q_c^{-1}$ plotted as a function of time for central and southern California (f is about 2 Hz). Stars indicate major earthquakes occurred within each study area. The number above each star is the magnitude.

sometimes, is not followed by a major earthquake, and some major earthquakes were not preceded by the pattern.

A rather surprisingly consistent observation made by studies is that coda Q^{-1} tends to take a minimum value during the period of high aftershock activity (GUSEV and LEMZIKOV, 1984; NOVELO-CASANOVA *et al.*, 1987; FAULKNER, 1988) except for the recent Northridge earthquake (OUYANG, 1994). Furthermore, TSUKUDA (1988) found in the epicentral area of the 1983 Misasa earthquake that a period of high coda Q^{-1} from 1977 to 1980 corresponds to a low rate of seismicity (quiescence). These observations suggest that the temporal change in coda Q^{-1} may be related primarily to creep fractures in the ductile part of lithosphere, rather than the shallower brittle part.

Several convincing cases were made also for the temporal correlation between coda Q^{-1} and b-value. The result was at first puzzling because the correlation was negative in some cases (AKI, 1985; JIN and AKI, 1986; ROBINSON, 1987) and positive in other cases (TSUKUDA, 1988; JIN and AKI, 1989). To resolve this puzzle, JIN and AKI (1989) proposed the creep model, in which creep fractures near the brittle-ductile transition zone of the lithosphere are assumed to have a characteristic size in a given seismic region. The increased creep activity in the ductile part would then increase the seismic attenuation in that part and at the same time produce

stress concentration in the upper brittle part favoring the occurrence of earthquakes with magnitude M_c corresponding to the characteristic size of the creep fracture. Then, if M_c is in the lower end of the magnitude range from which the b-value is evaluated the b-value would show a positive correlation with coda Q^{-1}, and if M_c is in the upper end, the correlation would be negative.

The creep model is consistent with the observed behaviors of coda Q^{-1} during the periods of aftershocks and quiescence mentioned earlier. Another support for the deeper source of the coda Q^{-1} change derives from the observed coincidence between a large increase in coda Q^{-1} in southern California during 1986–87 (PENG, 1989; JIN and AKI, 1989), and the increase in electrical conductivity in the same region (MADDEN *et al.*, 1993) which is attributed to the lower crust.

If the creep model is correct, the strongest correlation should be found between coda Q^{-1} and the seismicity of earthquakes with M_c, and the correlation should always be positive. Indeed, JIN and AKI (1993) found a remarkable positive correlation between coda Q^{-1} and the fraction of earthquakes in the magnitude range $M_c < M < M_c + 0.5$ for both central and southern California. Figure 12 shows the result for central California where the appropriate choice of M_c is 4.0. The correlation is highest (0.84) for the zero time lag and decays symmetrically with the time shift as shown in Figure 13. A very similar result is obtained for southern California as shown in Figure 14 where the appropriate choice of M_c is 3.0. The correlation is again the highest (0.81) at the zero time lag as shown in Figure 15.

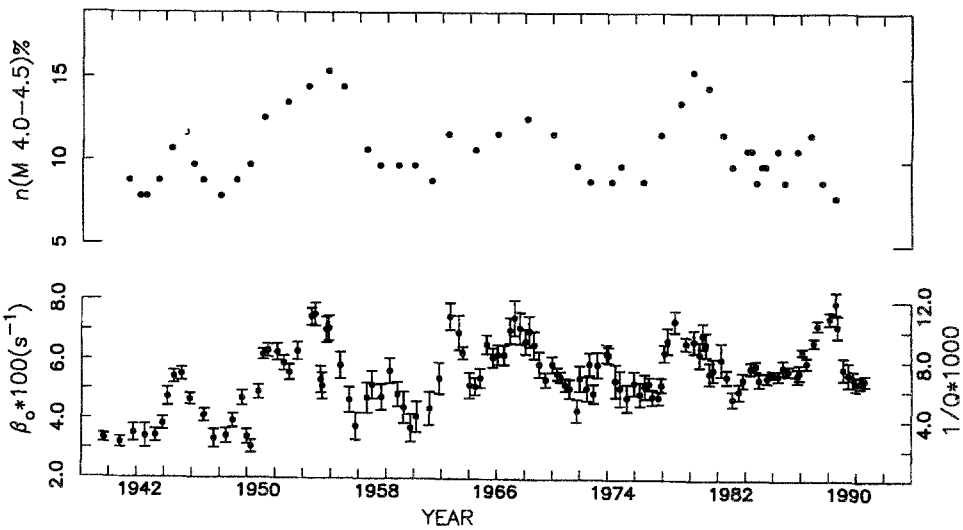

Figure 12
Comparison between temporal variation of $\pi f Q_c^{-1}$ (f is about 2 Hz) and fractional frequency of earthquakes with magnitude $4.0 \leq M \leq 4.5$, for central California, from JIN and AKI (1993).

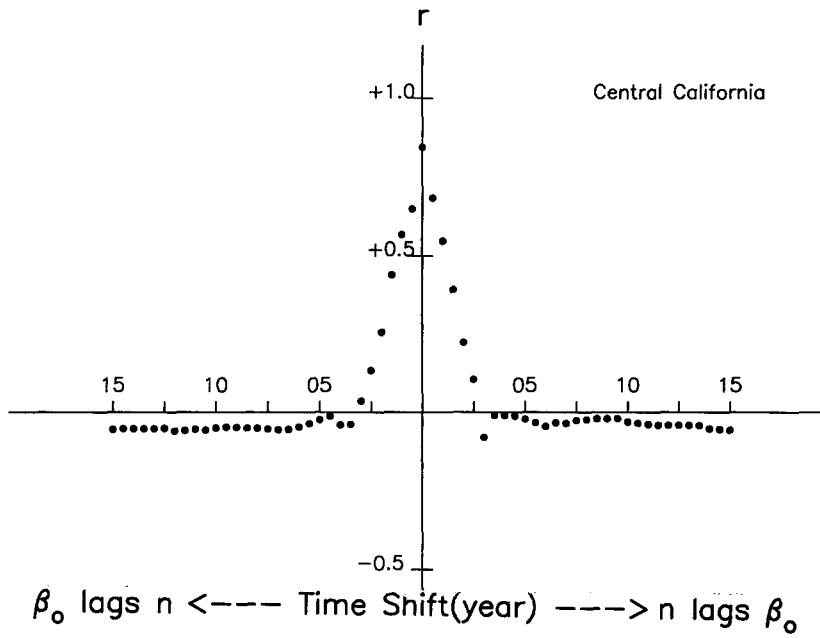

Figure 13
Cross-correlation function between the two time series shown in Figure 12.

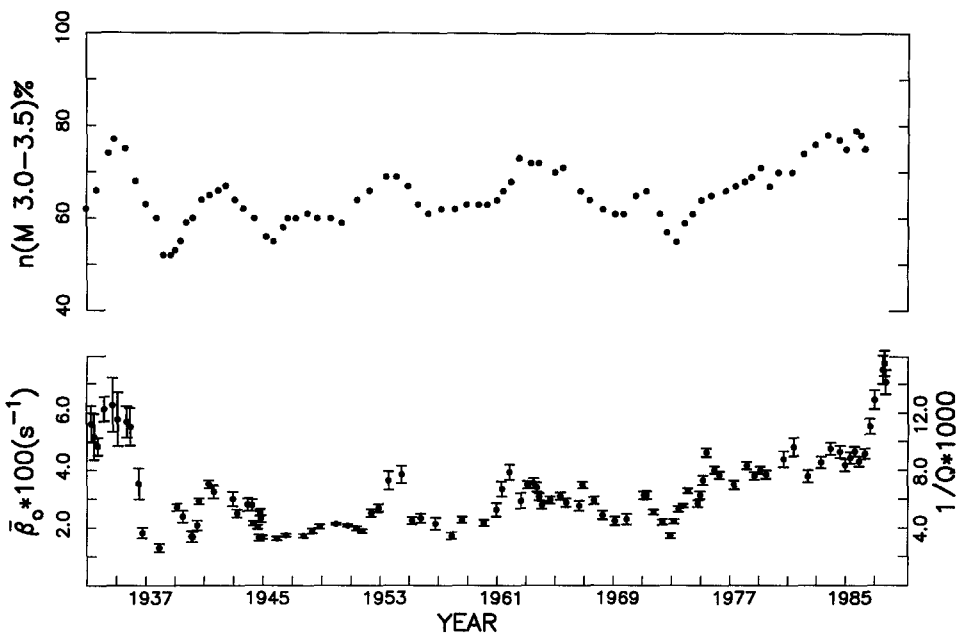

Figure 14
Comparison between temporal variations of $\pi f Q_c^{-1}$ (f is about 2 Hz) and fractional frequency of earthquakes with magnitude $3.0 \leq M \leq 3.5$, for southern California, from JIN and AKI (1993).

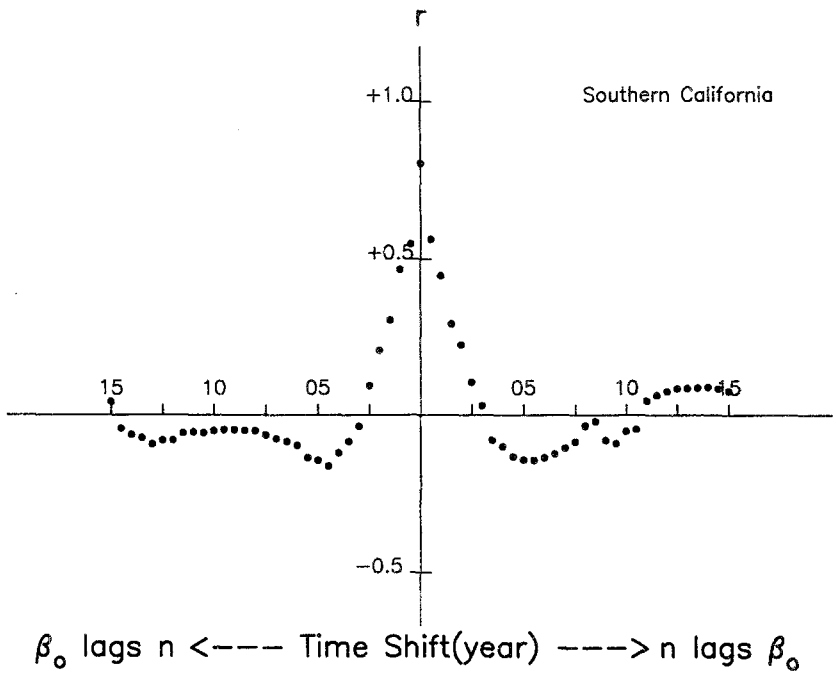

Figure 15
Cross-correlation function between the two time series shown in Figure 14.

Thus, our current working hypothesis is that the temporal change in coda Q^{-1} reflects the activity of creep fractures in the ductile part of lithosphere. The ductile part of lithosphere is larger than the brittle part. The deformation in the ductile part is the source of stress in the brittle part. Although we found that the coda Q^{-1} precursor is not reliable, the study of spatial and temporal variation in coda Q^{-1} may be still promising for understanding the loading process that leads to earthquakes in the brittle part.

Summary and Conclusions

In order to develop a predictive capability that will tell what will happen when a geologic fault with a known structure is subjected to a known stress condition, we searched for the scale-dependence in earthquake phenomena with the hope to find some structures in the earth that may control the earthquake processes. We found a hierarchy of length scales relevant to earthquake phenomena through observations related to (1) nucleation and stopping of fault rupture, (2) depth ranges of the brittle zone, (3) asperities and barriers distributed over a fault plane, (4) source-controlled f_{max}, (5) nonfractal behavior of creep events and (6) temporal correlation between the coda Q^{-1} and the fraction of earthquakes with the magnitude characteristic to a seismic region.

Our current working hypothesis is that the temporal change in coda Q^{-1} reflects the activity of creep fractures in the ductile part of lithosphere. We explain the observed positive correlation with seismicity (item (6) above) by assuming that creep fractures occur over cracks with a characteristic size (a few hundred meters in southern California), enhancing seismicity for earthquakes with the comparable size in the brittle part of lithosphere. Since the deformation in the ductile part is the source of stress in the brittle part, the existence of a unique size for creep fractures may give rise to other scale-dependent phenomena (e.g., items (4) and (5) above) as reviewed in the present paper. We hope that further testing of our working hypothesis may lead to better models of seismogenic structures and earthquake processes.

Acknowledgment

This work was supported by Southern California Earthquake Center under grants EAR–8920136 and USGS–14–08–0001–A0899. This is SCEC Contribution #122.

REFERENCES

AKI, K. (1968), *Seismic Displacement near a Fault*, J. Geophys. Res. *73*, 5359–5376.

AKI, K. (1969), *Analysis of the Seismic Coda of Local Earthquakes as Scattered Waves*, J. Geophys. Res. *74*, 6215–6231.

AKI, K. (1979), *Characterization of Barriers on an Earthquake Fault*, J. Geophys. Res. *84*, 6140–6148.

AKI, K. (1980), *Attenuation of Shear Waves in the Lithosphere for Frequencies from 0.05 to 25 Hz*, Phys. Earth Planet. Int. *21*, 50–60.

AKI, K., *Attenuation and scattering of short-period seismic waves in the lithosphere*. In *Identification of Seismic Sources—Earthquake or Underground Explosion* (eds. Husebye, E. S., and Mykkeltveit, S.) (D. Reidel Publishing Co. 1981) pp. 515–541.

AKI, K. (1983), *Strong Motion Seismology*, Proc. LXXXV course on *Earthquakes: Observation, Theory and Interpretation*, International School of Physics "Enrico Fermi", 223–250.

AKI, K. (1985), *Theory of Earthquake Prediction with Special Reference to Monitoring of the Quality Factor of Lithosphere by the Coda Method*, Earthq. Predict. Res. *3*, 219–230.

AKI, K. (1991), *Summary of Discussion on Coda Waves at the Istanbul IASPEI Meeting*, Phys. Earth Planet. Int. *67*, 1–3.

AKI, K. (1992a), *Higher Order Interrelations between Seismogenic Structures and Earthquake Processes*, Tectonophysics *211*, 1–12.

AKI, K. (1992b), *Scattering Conversions P to S versus S to P*, Bull. Seismol. Soc. Am. *82*, 1969–1972.

AKI, K., and PAPAGEORGIOU, A. S. (1989), *Separation of Source and Site Effects in Acceleration Power Spectra of Major California Earthquakes*, Proc. 9th World Conf. Earthquake Engineering *8*, 163–167.

AKI, K., and CHOUET, B. (1975), *Origin of Coda Waves: Source, Attenuation and Scattering Effects*, J. Geophys. Res. *80*, 3322–3342.

ALLEN, C. R., and NORDQUIST, J. M. (1972), *Foreshocks, Mainshock and Larger Aftershocks of the Borrego Mountain Earthquake*, U.S. Geol. Surv. Prof. Paper *787*, 16–23.

ANDERSON, J. G., and HOUGH, S. E. (1984), *A Model for the Shape of the Fourier Amplitude Spectrum of Acceleration at High Frequencies*, Bull. Seismol. Soc. Am. *74*, 1969–1993.

ARCHULETA, R. (1984), *A Faulting Model for the 1979 Imperial Valley, California Earthquake*, J. Geophys. Res. *89*, 4559–4585.

BAKUN, W. H., and MCEVILLY, T. V. (1984), *Recurrence Models and the Parkfield, California, Earthquakes*, J. Geophys. Res. *89*, 3051–3058.

BAKUN, W. H., STEWART, R. M., BUFE, C. G., and MARKS, S. M. (1980), *Implication of Seismicity for Failure of a Section of the San Andreas Fault*, Bull. Seismol. Soc. Am. *70*, 185–201.

BOLT, B. A. (1968), *The Focus of the 1906 California Earthquake*, Bull. Seismol. Soc. Am. *58*, 457–471.

BOORE, D. M. (1977), *Strong-motion Recordings of the California Earthquake of April 18, 1906*, Bull. Seismol. Soc. Am. *67*, 561–577.

BOUCHON, M. (1979), *Predictability of Ground Displacement and Velocity near and Earthquake Fault: An Example: The Parkfield Earthquake of 1966*, J. Geophys. Res. *84*, 6149–6156.

BOUCHON, M. (1982), *The Rupture Mechanism of the Coyote Lake Earthquake of 6 August 1979 Inferred from Near-field Data*, Bull. Seismol. Soc. Am. *72*, 745–757.

BRUHN, R. L., YONKEE, W. A., and PARRY, W. T. (1988), *Rupture Properties of Geometrical Boundaries in Extensional Faults Systems*, presented at the USGS Workshop on Fault Segmentation, 6–10 March, 1988, Palm Springs, CA.

BURFORD, R. O. (1988), *Retardations in Fault Creep Rates before Local Moderate Earthquakes along the San Andreas Fault System, Central California*, Pure and Appl. Geophys. *126*, 499–530.

BURK, C. A. (1965), *Geology of the Alaska Peninsula: Island Arc and Continental Margin*, Geol. Soc. Am. Mem. *99*, 147.

BUTLER, R., STEWART, G. S., and KANAMORI, H. (1979), *The July 27, 1976 Tangshan, China Earthquake: A Complex Sequence of Interplate Events*, Bull. Seismol. Soc. Am. *69*, 207–220.

CHEN, P., and NUTTLI, W. O. (1984a), *Estimates of Magnitude and Short-period Wave Attenuation of Chinese Earthquake for Modified Mercali Intensity Data*, Bull. Seismol. Soc. Am. *74*, 957–968.

CHEN, P., and NUTTLI, W. O. (1984b), *Estimates of Short-period Q Values and Seismic Moments from Coda Waves for Earthquakes of the Beijing and Yunnan Regions of China*, Bull. Seismol. Soc. Am. *74*, 1189–1208.

CHIN, B. H., and AKI, K. (1991), *Simultaneous Study of the Source, Path and Site Effects on Strong Ground Motion during the 1989 Loma Prieta Earthquake: A Preliminary Result on Pervasive Non-linear Site Effects*, Bull. Seismol. Soc. Am. *81*, 1859–1884.

CHOUET, B. (1979), *Temporal Variation in the Attenuation of Earthquake Coda near Stone Canyon, Calif.*, Geophys. Res. Lett. *6*, 143–146.

CLARK, M. M. (1972), *Surface Rupture along the Coyote Creek Fault*, U.S. Geol. Surv. Prof. Paper *787*, 55–86.

CROSSON, R. S., MARTINI, M., SCARPA, R., and KEY, S. C. (1986), *The Southern Italy Earthquake of 23 November 1980: An Unusual Pattern of Faulting*, Bull. Seismol. Soc. Am. *76*, 381–394.

DAS, S., and AKI, K. (1977), *Fault Planes with Barriers: A Versatile Earthquake Model*, J. Geophys. Res. *82*, 5648–5670.

DEL PEZZO, IANNACCONE, E. G., MARTINI, M., and SCARPA, R. (1983), *The 23 November 1980 Southern Italy Earthquake*, Bull. Seismol. Soc. Am. *73*, 187–200.

DESCHAMPS, A., and KING, G. C. P. (1983), *The Campania-Lucanic (Southern Italy) Earthquake of 23 November, 1980*, Earth Planet. Sci. Lett. *62*, 296–304.

DESCHAMPS, A., GAUDEMER, Y., and CISTERNAS, A. (1982), *The El Asnam, Algeria, Earthquake of 10 October 1980: Multiple-source Mechanism Determined from Long-period Records*, Bull. Seismol. Soc. Am. *72*, 1111–1128.

DEWEY, J. W. (1976), *Seismicity of Northern Anatolia*, Bull. Seismol. Soc. Am. *66*, 843–868.

EATON, J. P., O'NEILL, M. E., and MURDOCK, J. N. (1970), *Aftershocks of the 1966 Parkfield-Cholame, California Earthquake: A Detailed Study*, Bull. Seismol. Soc. Am. *60*, 1151–1197.

FAULKNER, J. (1988), *Temporal Variation of Coda Q*, MS Thesis, University of Southern California, Los Angeles.

FRANKEL, A., and CLAYTON, R. W. (1986), *Finite Difference Simulations of Seismic Scattering: Implications for the Propagation of Short-period Seismic Waves in the Crust and Models of Crust Heterogeneity*, J. Geophys. Res. *91*, 6465–6489.

GAO, L. S., and AKI, K. (1995), *Effect of Finite Thickness of Scattering Layer on Coda Q of Local Earthquakes*, J. Geodynamics, in press.

GAO, L. S., LEE, L. C., BISWAS, N. N., and AKI, K. (1983), *Comparison of the Effects between Single and Multiple Scattering on Coda Waves for Local Earthquakes*, Bull. Seismol. Soc. Am. *73*, 377–390.

GUSEV, A. A. (1992), personal communication.

GUSEV, A. A., and LEMZIKOV, V. K. (1984), *The Anomalies of Small Earthquake Coda Wave Characteristics before the Three Large Earthquakes in the Kuril-Kamchatka Zone (in Russian)*, Vulk. Seismol., *4*, 76–90.

HAGHIPOUR, A., and AMIDI, M. (1980), *The November 14 to December 25, 1979 Chaenat Earthquakes of Northeast Irand and their Tectonic Implications*, Bull. Seismol. Soc. Am. *70*, 1751–1757.

HANKS, T. C. (1982), f_{max}, Bull. Seismol. Soc. Am. *72*, 1867–1879.

HARTZELL, S. (1980), *Faulting Process of the May 17, 1876 Gazli, USSR Earthquake*, Bull. Seismol. Soc. Am. *70*, 1651.

HARTZELL, S. H., and HEATON, T. H. (1986), *Rupture History of the 1984 Morgan Hill, California, Earthquake from the Inversion of Strong Motion Records*, Bull. Seismol. Soc. Am. *76*, 649–674.

HERRAIZ, M., and ESPINOSA, A. F. (1987), *Coda Waves: A Review*, Pure and Appl. Geophys. *125*, 499–577.

HONDA, S., and UYEDA, S., *Thermal process in subduction zones, A review and preliminary approach on the origon of arc volcanism.* In *Arc Volcanism, Physics and Tectonics*, (D. Shimozura, and I. Yokoyama, eds.) (TERRAPUB, Tokyo 1983) pp. 117–140.

HOSHIBA, M. (1993), *Separation of Scattering Attenuation and Intrinsic Absorption in Japan with the Multiple Lapse Time Window Analysis from Full Seismogram Envelope*, J. Geophys. Res. *98*, 15809–15824.

HOSHIBA, M., SATO, H., and FEHLER, M. (1991), *Numerical Basis of the Separation of Scattering and Intrinsic Absorption from Full Seismogram Envelope: A Monte-Carlo Simulation of Multiple Isotropic Scattering*, Pap. Meterol. Geophys. *42*, 65–91.

IRIKURA, K., and YOKOI, T. (1984), *Scaling Law of Seismic Source Spectra for the Aftershocks of 1983 Central Japan Sea Earthquake*, Abstract, Seismological Society of Japan.

JENNINGS, C. W. (1975), *Fault Map of California*, Williams and Heintz Map Corp., Capitol Heights, MD.

JIN, A., and AKI, K. (1986), *Temporal Changes in Coda Q before the Tangshan Earthquake of 1976 and the Haicheng Earthquake of 1975*, J. Geophys. Res. *91*, 665–673.

JIN, A., and AKI, K. (1988), *Spatial and Temporal Correlation between Coda Q and Seismicity in China*, Bull. Seismol. Soc. Am. *78*, 741–769.

JIN, A., and AKI, K. (1989), *Spatial and Temporal Correlation between Coda Q^{-1} and Seismicity and its Physical Mechanism*, J. Geophys. Res. *94*, 14041–14059.

JIN, A., and AKI, K. (1993), *Temporal Correlation between Coda Q^{-1} and Seismicity—Evidence for a Structural Unit in the Brittle-ductile Transition Zone*, J. Geodyn. *17*, 95–120.

JIN, A., MAYEDA, K., ADAMS, D., and AKI, K. (1994), *Separation of Intrinsic and Scattering Attenuation in Southern California Using TERRAscope Data*, J. Geophys. Res. *99*, 17,835–17,848.

KANAMORI, H. (1970), *The Alaska Earthquake of 1964: Radiation of Long-period Waves and Source Mechanism*, J. Geophys. Res. *75*, 5029–5040.

KANAMORI, H. (1978), *Quantification of Earthquakes*, Nature *271*, 411–414.

KANAMORI, H., and STEWART, G. S., (1978), *Seismological Aspects of the Guatemala Earthquake of 4 February 1976*, J. Geophys. Res. *83*, 3427–3434.

KELLEHER, J., and SAVINO, J. (1975), *Distribution of Seismicity before Large Strike-slip and Thrust-type Earthquakes*, J. Geophys. Res. *80*, 260–271.

KINOSHITA, S. (1992), *Local Characteristics of the f_{max} of Bedrock Motion in Tokyo Metropolitan Area*, J. Phys. Earth *40*, 487–515.

LEARY, P. C., LI, Y.-G., and AKI, K. (1987), *Observation and Modeling of Fault Zone Fracture Seismic Anisotropy, I, P, SV, SH Travel Times*, Geophys. J. R. Astron. Soc. *91*, 461–484.

LI, Y.-G., and LEARY, P. C. (1990), *Fault Zone Trapped Seismic Waves*, Bull. Seismol. Soc. Am. *80*, 1245–1271.

LI, Y.-G., AKI, K., ADAMS, D., and HASEMI, A. (1994a), *Seismic Guided Waves Trapped in the Fault Zone of the Landers, California, Earthquake of 1992*, J. Geophys. Res. *99*, 11,705–11,722.

LI, Y.-G., VIDALE, J. E., AKI, K., MARONE, C. J. and LEE, W. H. K. (1994b), *Fine Structure of the Landers Fault Zone: Segmentation and the Rupture Process*, Science *265*, 367–370.

LI, Y.-G., LEARY, P. C., AKI, K., and MALIM, P. E. (1990), *Seismic Trapped Modes in the Oroville and San Andreas Fault Zones*, Science *249*, 763–766.

LINDH, A. G., and BOORE, D. M. (1981), *Control of Rupture by Fault Geometry during the 1966 Parkfield Earthquake*, Bull. Seismol. Soc. Am. *71*, 95–116.

MADDEN, T. R., LATORRACA, G. A., and PARK, S. K. (1993), *Electrical Conductivity Variations around the Palmdale Section of the San Andreas Fault Zone*, J. Geophys. Res. *98*, 795–808.

MATSUNAMI, K. (1991), *Laboratory Tests of Excitation and Attentuation of Coda Waves using 2-D Models of Scattering Media*, Phys. Earth Planet. Int. *67*, 104–114.

MAYEDA, K., KOYANAGI, S., HOSHIBA, M., AKI, K., and ZENG, Y. (1992), *A Comparative Study of Scattering, Intrinsic and Coda Q^{-1} for Hawaii, Long Valley, and Central California between 1.5 and 15 Hz*, J. Geophys. Res. *97*, 6643–6659.

NICHOLSON, C. (1988), *Fault Interaction and Segmentation along the San Andreas Fault System, Southern California*, presented at the USGS Workshop on Fault Segmentation, 6–10 March, 1988, Palm Springs, CA.

NOVELO-CASANOVA, D. A., BERG, E., HSU, Y., and HELSLEY, C. E. (1985), *Time-space Variation Seismic S-wave Coda Attenuation (Q^{-1}) and Magnitude Distribution (b-values) for the Petatlan Earthquake*, Geophys. Res. Lett. *12*, 789–792.

OUYANG, H. (1994), personal communication.

PAPAGEORGIOU, A. S. (1988), *On Two Characteristic Frequencies of Acceleration Spectra: Patch Corner Frequency and f_{max}*, Bull. Seismol. Soc. Am. *78*, 509–529.

PAPAGEORGIOU, A. S., and AKI, K. (1983), *A Specific Barrier Model for the Quantitative Description of Inhomogeneous Faulting and the Prediction of Strong Motion, Part I. Description of the Model*, Bull. Seismol. Soc. Am. *73*, 693–722, *Part II. Applications of the Model*, Bull. Seismol. Soc. Am. *73*, 953–978.

PENG, J. Y. (1989), *Spatial and Temporal Variation of Coda Q^{-1} in California*, Ph.D. Thesis, University of Southern California, Los Angeles.

PHILLIPS, W. S., and AKI, K. (1986), *Site Amplification of Coda Waves from Local Earthquakes in Central California*, Bull. Seismol. Soc. Am. *76*, 627–643.

PLAFKER, G., BONILLA, M. G., and BONIS, S. B. (1976), *Geologic Effects, The Guatemala Earthquake of 4 February 1976*, U.S. Geol. Surv. Prof. Paper *1002*, 38–51.

RAUTIAN, T. G., and KHALTURIN, V. I. (1978), *The Use of Coda for Determination of the Earthquake Source Spectrum*, Bull. Seismol. Soc. Am. *68*, 923–948.

REASENBERG, P., and ELLSWORTH, W. L. (1982), *Aftershocks of the Coyote Lake, California, Earthquake of 6 August 1979: A Detailed Study*, J. Geophys. Res. *87*, 10637–10655.

RICHTER, C. F., (1958), *Elementary Seismology* (W. H. FREEMAN, San Francisco), 768 pp.

ROCA, A. (1990), *Determination del camp proximo de terremotos por redes de aceleragrafos*, Doctor en Ciencias Fisicas, Universidad Complutense de Madrid.

RUFF, L., and KANAMORI, H. (1980), *Seismicity and the Subduction Process*, Phys. Earth Planet. Int. *23*, 240–252.

SABINE, W. C. *Collected Papers on Acoustics* (Harvard University Press, Cambridge, Mass. 1922).

SATO, H. (1982a), *Amplitude Attenuation of Impulsive Waves in Random Media Based on Travel Time Corrected Mean Wave Formalism*, J. Acoust. Soc. Am. *71*, 559–564.

SATO, H. (1982b), *Attenuation of S Waves in the Lithosphere due to Scattering by its Random Velocity Structure*, J. Geophys. Res. *87*, 7779–7785.

SATO, H. (1986), *Temporal Change in Attenuation Intensity Before and After Eastern Yamanashi Earthquake of 1983, in Central Japan*, J. Geophys. Res. *91*, 2049–2061.

SATO, H. (1988), *Temporal Change in Scattering and Attenuation Associated with the Earthquake Occurrence—A Review of Recent Studies on Coda Waves*, Pure and Appl. Geophys. *126*, 465–498.

SCHWARTZ, D. P., and COPPERSMITH, K. J. (1984), *Fault Behavior and Characteristic Earthquakes: Examples from the Wasatch and San Andreas Fault Zones*, J. Geophys. Res. *89*, 5681–5698.

ROBINSON, R. (1987), Pure and Appl. Geophys. *125*, 579–596.

SEGALL, P., and DUS, Y. (1993), *How Similar Were the 1934 and 1966 Parkfield Earthquakes?* J. Geophys. Res. *98*, 4527–4538.

SHANG, T., and GAO, L. S. (1988), *Transportation Theory of Multiple Scattering and its Application to Seismic Coda Waves of Impulse Source*, Sci. Sinica, Series B *31*, 1503–1514.

SHARP, R. V., LIENKAEMPER, J. J., BONILLA, M. G., BURKE, D. B., FOX, B. F., HERD, D. G., MILLER, D. M., MORTON, D. M., PONTI, D. J., RYMER, M. J., TINLEY, J. C., YOUNT, J. C., KAHLE, J. E., HART, E. W., and SIEH, K. E. (1982), *Surface Faulting in the Central Imperial Valley, The Imperial Valley, California, Earthquake of 15 October 1979,* U.S. Geol. Surv. Prof. Paper *1254,* 119–144.

SHIMAMOTO, T., SENO, T., and UYEDA, S. (1993), *A simple rheological framework for comparative subductology.* In *Relating Geophysical Structures and Processes; The Jeffreys Volume* (eds. Aki, K., and Dmowska, R.) (American Geophysical Union, Geophysical Monograph *76*), 39–52.

SHIMAZAKI, K. (1986), *Small and large earthquakes: The effects of the thickness of seismogenic layer and the free surface.* In *Earthquake Source Mechanics* (eds. Das, S., Boatwright, J., and Scholz, C. H.) (Geophys. Mono. *37,* M. Ewing Series), 209–216.

SHIMAZAKI, K., and SOMERVILLE, P. (1979), *Static and Dynamic Parameters of the Izu-Oshima, Japan Earthquake of* 14 *January 1978,* Bull. Seismol. Soc. Am. *69,* 1343–1378.

SIEH, K. E. (1978a), *Central California Foreshocks of the Great 1857 Earthquake,* Bull. Seismol. Soc. Am. *68,* 1731–1749.

SIEH, K. E. (1978b), *Slip along the San Andreas Fault Associated with the Great 1857 Earthquake,* Bull. Seismol. Soc. Am. *68,* 1421–1448.

SINGH, S. K., and HERRMANN, R. B. (1983), *Regionalization of Crustal Coda Q in the Continental United States,* J. Geophys. Res. *88,* 527–538.

STEINBRUGGE, K. V., ZACHER, E. G., TOCHER, D., WHITTEN, C. A., and CLAIR, C. N. (1960), *Creep on the San Andreas Fault,* Bull. Seismol. Soc. Am. *50,* 389–415.

SU, F., and AKI, K. (1990), *Spatial and Temporal Variation in Coda* Q^{-1} *Associated with the North Palm Springs Earthquake of 1986,* Pure and Appl. Geophys. *133,* 23–52.

SU, F., AKI, K., and BISWAS, N. N. (1991), *Discriminating Quarry Blasts from Earthquakes Using Coda Waves,* Bull. Seismol. Soc. Am. *81,* 162–178.

SU, F., AKI, K., TENG, T., ZENG, Y., KOYANAGI, S., and MAYEDA, K. (1992), *The Relation between Site Amplification Factor and Surficial Geology in Central California,* Bull. Seismol. Soc. Am. *82,* 580–602.

TOCHER, D. (1960), *Creep on the San Andreas Fault—Creep Rate and Related Measurements at Vinyard, California,* Bull. Seismol. Soc. Am. *50,* 396–404.

TSUJIURA, M. (1978), *Spectral Analysis of the Coda Waves from Local Earthquakes,* Bull. Earthq. Res. Inst., Tokyo Univ. *53,* 1–48.

TSUKUDA, T. (1988), *Coda Q before and after the 1983 Misasa Earthquake of M 6.2, Tottori Pref., Japan,* Pure and Appl. Geophys. *128,* 261–280.

WU, R. S. (1982), *Attenuation of Short-period Seismic Waves due to Scattering,* Geophys. Res. Lett. *9,* 9–12.

WU, R. S. (1985), *Multiple Scattering and Energy Transfer of Seismic Waves—Separation of Scattering Effect from Intrinsic Attenuation, I. Theoretical Modeling,* Geophys. J. R. Astron. Soc. *82,* 57–80.

YIELDING, G., JACKSON, J. A., KING, G. C. P., SIVHAL, H., BITA-GINZI, C., and WOOD, R. M. (1982), *Relations between Surface Deformation, Fault Geometry, Seismicity and Rupture Characteristics during the El Asnam Earthquake of 10 October 1980,* Earth Planet. Sci. Lett. *56,* 287–304.

ZENG, Y. (1993), *Theory of Scattered P and S Waves Energy in a Random Isotropic Scattering Medium,* Bull. Seismol. Soc. Am. *83,* 1264–1277.

ZENG, Y., SU, F., and AKI, K. (1991), *Scattering Wave Energy Propagation in a Medium with Randomly Distributed Isotropic Scatterers, 1. Theory,* J. Geophys. Res. *96,* 607–619.

(Received September 20, 1994; revised March 28, 1995, accepted April 14, 1995)